PROJECT: Saffman Taylor Instability

CL326: Integrated Chemical Lab - I

Gaurav Budhwani
2211085
Chemical Engineering

Garima Nama
22110084
Chemical Engineering

Durgam Rachana
22110079
Chemical Engineering

Professor

Karthik Subramaniam Pushpavanam

November 25, 2024

Contents

1 Introduction . . . 2
2 Objective . . . 3
3 Literature Review . . . 3
3.1 Applications and Real-World Relevance . . . 4
4 Experimental System Description . . . 5
4.1 Experimental Setup . . . 5
4.2 Principles Behind the System . . . 7
4.3 Observations and Analysis . . . 8
4.4 Modifications and Improvements . . . 9
4.5 Schematic Diagram and Workflow . . . 10
5 Modeling Approach . . . 10
5.1 Analytical Modeling[1] . . . 10
5.2 Numerical Modeling[1] . . . 12
5.3 Diffusion-Limited Aggregation (DLA) Modeling [2] . . . 14
5.4 Why We Use DLA Instead of Normal Algorithms . . . 14
6 Results and Analysis . . . 15
6.1 Fingering Patterns . . . 15
6.2 Interface Evolution . . . 15
6.3 Critical Parameters . . . 15
6.4 Numerical Outputs . . . 15
7 Sensitivity Analysis . . . 16
7.1 DLA Simulation Sensitivity Analysis . . . 19
7.2 Comparison of Sensitivity Across Models . . . 22
8 Discussions and Conclusion . . . 23
8.1 Key Insights . . . 23
8.2 Challenges and Limitations . . . 23
8.3 Potential Improvements . . . 23
9 Future Work . . . 24
9.1 Model Refinement . . . 24
9.2 Experimental Enhancements . . . 24
9.3 Alternative Approaches . . . 24
1 Simulation Codes . . . 27
1.1 Code for Modelling and Simulation Using Algorithm from Research Paper . . . 27
1.2 Code for Modelling and Simulation Using DLA Algorithm 28

1 Introduction

The Saffman-Taylor instability, often referred to as viscous fingering, is a phenomenon observed when a less viscous fluid displaces a more viscous one in a confined geometry, such as a Hele-Shaw cell. This instability is of significant interest in various scientific and engineering disciplines due to its implications in fluid mechanics, porous media flow, and real-world applications like enhanced oil recovery and CO sequestration. The phenomenon produces intricate "fingering" patterns at the fluid interface, which are a direct result of the interplay between viscous forces, surface tension, and system perturbations.

This project aims to investigate the Saffman-Taylor instability through theoretical analysis, experimental observations, and numerical simulations. By employing a Hele-Shaw cell as the experimental framework, the study replicates the interface dynamics under controlled conditions. The Hele-Shaw setup consists of two parallel plates separated by a narrow gap, which effectively reduces the problem to two dimensions. The introduction of a less viscous fluid, such as air or water, into a more viscous medium like glycerol results in a displacement process that amplifies instabilities at the interface, forming characteristic "fingers."

The theoretical framework for understanding this phenomenon is grounded in Darcy's law, which describes the flow of fluids through porous media and thin gaps under laminar conditions. The derivation of Darcy's law from the Navier-Stokes equations simplifies the complex dynamics of the Hele-Shaw flow by incorporating assumptions of uniformity and negligible inertial effects. Additionally, the role of the Laplace-Young boundary condition, which relates pressure difference to surface tension and curvature, is critical in describing the interface's evolution.

To further quantify the instability, the Capillary number (Ca) is introduced, representing the ratio of destabilizing viscous forces to stabilizing surface tension. High Capillary numbers correspond to stronger instabilities and more pronounced fingering patterns. Through linear stability analysis, the growth of perturbations on the interface is mathematically characterized, identifying conditions under which perturbations grow or decay. This provides insight into how parameters such as injection velocity and surface tension influence the resulting patterns.

Numerical simulations complement the theoretical and experimental efforts by providing a computational perspective on the instability's dynamics. Using finite difference methods and iterative solvers for Laplace's equation, simulations model the pressure field and interface evolution over time. Despite challenges with long-term accuracy due to computational limitations, these simulations offer valuable verification of theoretical predictions and initial experimental conditions.

2 Objective

The objective of this study is to analyze the *Saffman-Taylor instability* through theory, experimentation, and numerical simulations. The aims are:

1. **Theoretical Analysis:** Derive the governing equations, such as Darcy's Law, and perform linear stability analysis to understand the growth and decay of interface perturbations.
2. **Experimental Observation:** Use a Hele-Shaw cell to observe the instability, document the formation of fingering patterns, and study the effects of injection rate, surface tension, and viscosity.
3. **Numerical Simulation:** Model the pressure field and interface evolution using computational methods and validate against experimental results.
4. **Applications:** Explore the practical implications of the instability in fields like enhanced oil recovery and fluid displacement in porous media.

3 Literature Review

The Saffman-Taylor instability, also known as viscous fingering, arises when a less viscous fluid displaces a more viscous fluid within a confined geometry, such as a Hele-Shaw cell. This phenomenon is significant in applications like enhanced oil recovery and environmental management. The instability's progression depends on factors like viscosity contrasts, surface tension, and pressure gradients, which cause intricate finger-like patterns to form at the fluid interface.

Theoretical insights[10] into viscous fingering derive from Darcy's law, which governs the flow of viscous fluids through porous media. In Hele-Shaw flow, this is expressed as:

$$\mathbf{u} = -\frac{h^2}{12\mu}\nabla P, \tag{1}$$

where h is the plate spacing and μ is the fluid viscosity. This relationship models the flow velocity as a function of pressure gradients, forming the basis for theoretical and numerical studies.

Linear stability analysis is a key method to understand this instability. The equation for the growth rate (σ) of disturbances is:

$$\sigma = \frac{k\Delta P - \gamma k^3}{\mu_1 + \mu_2}, \tag{2}$$

where k is the wavenumber, ΔP is the pressure difference, γ is surface tension, and μ_1, μ_2 are the viscosities of the fluids. This analysis shows that surface tension stabilizes the interface, especially for short wavelengths.

Experiments validate these theories by injecting a less viscous fluid into a more viscous one within a Hele-Shaw cell. Observations reveal how changes in

fluid properties, injection rates, and gap sizes influence the fingering patterns. For example, increasing the viscosity contrast amplifies instability, while higher surface tension dampens it. The capillary number (Ca), defined as:

$$\text{Ca} = \frac{\mu U}{\gamma}, \tag{3}$$

quantifies the relationship between viscous forces and surface tension. Larger Ca values indicate dominant viscous forces, leading to more pronounced fingering.

Hele-Shaw cells are widely employed to experimentally study the Saffman-Taylor instability. Typically, a less viscous fluid, such as air or water, is injected into a more viscous medium, like glycerol. The experiments demonstrate how flow rate, fluid viscosity, and interfacial tension govern pattern morphology. For instance, increasing the injection speed (flow rate) generates thinner, more numerous fingers due to higher destabilizing forces.

Modifications to the Hele-Shaw setup, such as altering plate gaps or using fluids with varying viscosities, reveal quantitative relationships between experimental conditions and finger geometry. These experiments validate analytical models, showing consistency with theoretical predictions like critical wavelength and growth rates of perturbations.

Numerical approaches[9], like the Volume of Fluid (VOF) method, model complex interactions in viscous fingering. Advanced simulations use the Oldroyd-B model to incorporate viscoelastic effects:

$$\nabla \cdot \mathbf{p} + \lambda \frac{\partial \mathbf{p}}{\partial t} = 2\mu_p \mathbf{D}, \tag{4}$$

where $\mathbf{p}$ is polymeric stress, λ is relaxation time, and $\mathbf{D}$ is the deformation rate tensor. These simulations reveal that elasticity in the displacing fluid can stabilize the interface by increasing extensional viscosity, reducing the growth of fingers.

Viscoelastic fluids exhibit unique behavior compared to Newtonian fluids. Research shows that increasing the elasticity number (En) or capillary number stabilizes the interface. In contrast, a higher viscosity ratio ($R = \mu_2/\mu_1$) destabilizes the flow, leading to more irregular patterns. These findings have direct implications for oil recovery and fluid mixing in industrial processes.

3.1 Applications and Real-World Relevance

1. **Enhanced Oil Recovery:** Fingering instability significantly affects oil recovery by influencing the displacement efficiency of water or gas injected into oil reservoirs. Understanding this instability helps optimize injection strategies.

2. **Microfluidics:** Hele-Shaw cells mimic the behavior of microfluidic systems. Controlling instability improves precision in applications like droplet generation and lab-on-chip devices.

3. **Environmental Management:** The Saffman-Taylor instability helps predict pollutant migration in porous media, aiding in contamination control and groundwater remediation.

The Saffman-Taylor instability is a cornerstone of fluid mechanics, linking theoretical principles, experimental insights, and computational models to real-world applications. Analytical models provide a foundational understanding, while numerical simulations and experiments deepen our knowledge of fluid behavior in confined systems. Future studies on non-Newtonian fluids and advanced simulations promise further advancements, particularly in industrial and environmental domains.

4 Experimental System Description

The experiment aims to study the Saffman-Taylor instability, which occurs when a less viscous fluid (dye water) displaces a more viscous fluid (like glycerol) in a confined setup. This displacement creates patterns called fingers at the interface of the two fluids. This phenomenon is explored using a Hele-Shaw cell to understand the physical principles of interfacial instability and its dependence on various parameters like flow rate, viscosity, and surface tension.

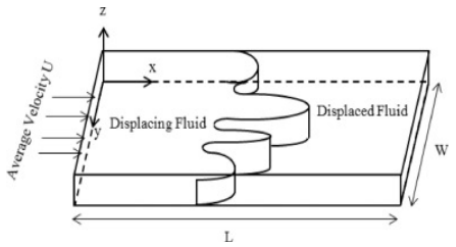

Figure 1: Hele-Shaw Cell [8]

4.1 Experimental Setup

Hele-Shaw Cell:

- A Hele-Shaw cell is a simple setup with two flat plates placed parallel to each other with a very small gap between them, typically 0.1–0.5 mm.

Hele-Shaw Cell Design:

- Two parallel acrylic sheets are used to create a thin, uniform gap.
- Small spacers (e.g., transparency films) are placed between the plates to maintain a consistent gap, typically 0.1–0.5 mm.

Figure 2: Apparatus for performing the experiment.

- A hole is drilled at the center of the top plate to inject the less viscous fluid.

This setup confines the flow into a thin, two-dimensional (2D) space, making it easier to observe and study the Saffman-Taylor instability.

Fluids Used:

Figure 3: Fluids Used (Glycerol and Food Dye)

- **More viscous fluid:** Glycerol, chosen for its high viscosity, which creates a strong contrast with the displacing fluid.
- **Less viscous fluid:** Colored water or air, used to displace glycerol and make the interface more visible.

The fluids are carefully filtered to remove impurities that could distort the patterns.

- Used an adequate amount of colored liquid instead of a small amount to ensure proper displacement of glycerol and better pattern formation.
- Reduced the amount of glycerol between the sheets from excessive to just enough for even spreading.
- Removed air bubbles from the glycerol to prevent irregular patterns.
- Used a syringe needle for injection instead of a wider tube to ensure smoother and more controlled flow.

4.2 Principles Behind the System

The Saffman-Taylor instability is governed by several key physical principles, primarily the interplay between viscosity, surface tension, and flow dynamics:

1. **Viscosity Contrast:** The instability occurs when a more viscous fluid (glycerol) is displaced by a less viscous fluid (water or air). This contrast leads to the formation of instabilities at the interface, as the less viscous fluid is able to push into the more viscous fluid, creating fingers. The greater the viscosity contrast, the more pronounced the fingering patterns become.
2. **Surface Tension:** Surface tension acts as a stabilizing force at the interface between the two fluids. Small disturbances at the interface are suppressed by surface tension, while larger disturbances grow into fingers as the destabilizing viscous forces take over. The Laplace-Young equation governs the pressure difference across the interface, which is dependent on the curvature of the interface and the surface tension:
$$P_{\text{inner}} - P_{\text{outer}} = \gamma\kappa,$$
where γ is the surface tension and κ is the curvature of the interface.
3. **Darcy's Law:** The flow of fluid in the Hele-Shaw cell is governed by Darcy's Law:
$$\mathbf{u} = -\frac{1}{\mu}\nabla P,$$
where $\mathbf{u}$ is the velocity, μ is the viscosity, and ∇P is the pressure gradient. This law describes the flow of fluids through porous media and helps predict the flow patterns observed during the experiment.
4. **Capillary Number (Ca):** The capillary number is the ratio of viscous forces to surface tension forces and is given by:
$$\text{Ca} = \frac{\mu U}{\sigma},$$
where U is the velocity of the less viscous fluid, and σ is the surface tension. Higher capillary numbers lead to more pronounced instability and thinner fingers, as viscous forces dominate over surface tension.

The observed results were consistent with theoretical predictions. The critical wavelength (the size of the fingers) was found to be dependent on the flow rate, with smaller fingers forming at higher flow rates and larger fingers at slower injection speeds. The capillary number was also calculated, and the experimental results showed a clear relationship between the capillary number and the development of the instability.

4.3 Observations and Analysis

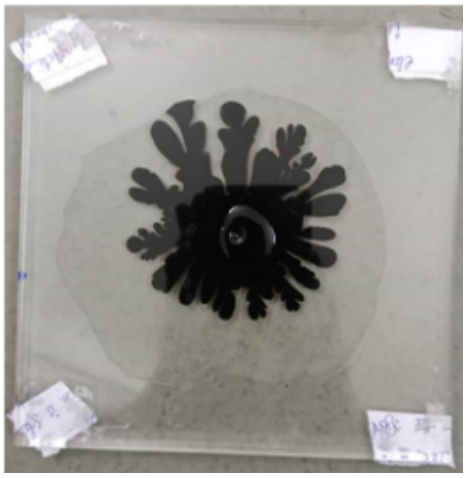

Figure 4: Saffman Taylor Instability (finger patterns)

Fingering Patterns :

- Slow injection created wider and fewer fingers.
- Faster injection led to thinner and more numerous fingers.
- Patterns were irregular when the setup was imperfect (e.g.uneven gaps or air bubbles).

Challenges and Unexpected Results :

- Irregular or unclear patterns due to:
    1. Uneven plate spacing.
    2. Impurities or air bubbles in the fluids.
    3. Inconsistent injection rates when using a manual syringe.
- Patterns collapsing at very slow injection rates due to high surface tension.

4.4 Modifications and Improvements

To improve the accuracy and repeatability of the experiment, the following modifications are planned:

- Adjusted the gap between the sheets from a large gap to a very thin and even gap to help form clear patterns.
- Changed the injection speed:
    1. Reduced from very fast injection, which caused the colored liquid to exit quickly without entering the glycerol.
    2. Avoided very slow injection, which produced unclear patterns.
    3. Maintained a steady, moderate speed to allow the colored liquid to mix properly with the glycerol and form distinct patterns.
    4. When injecting manually, we ensured the syringe movement is as smooth and consistent as possible. Sudden jerks or variations in injection speed can disturb the interface.
- Used an adequate amount of colored liquid instead of a small amount to ensure proper displacement of glycerol and better pattern formation.
- Reduced the amount of glycerol between the sheets from excessive to just enough for even spreading. Removed air bubbles from the glycerol to prevent irregular patterns.
- Used a syringe needle for injection instead of a wider tube to ensure smoother and more controlled flow.

4.5 Schematic Diagram and Workflow

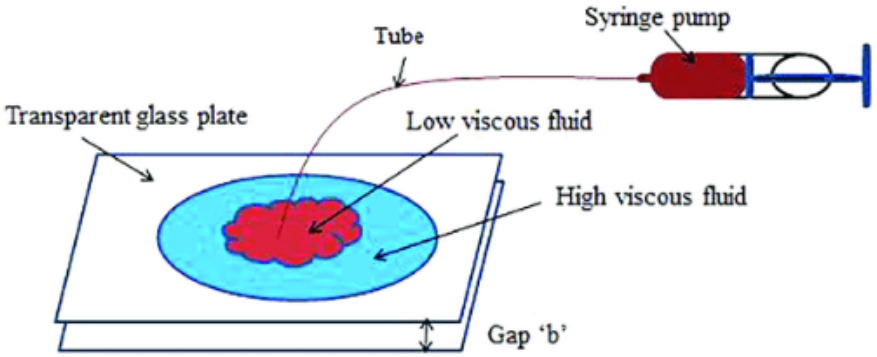

Figure 5: Schematic Diagram of the Experimental Setup for Saffman-Taylor Instability

Workflow:

1. Assemble the Hele-Shaw cell carefully, ensuring the plates are flat and the gap is uniform.
2. Fill the cell with glycerol, ensuring no air bubbles are trapped.
3. Use the syringe to inject colored water or air at a controlled flow rate through the central hole.
4. Record the interface evolution using the camera.
5. Adjust the flow rate incrementally to observe the effect on fingering patterns.
6. Measure parameters like finger width, growth rate, and critical wavelength from the recordings.
7. Compare experimental patterns with theoretical predictions.

5 Modeling Approach

5.1 Analytical Modeling[1]

The analytical approach to modeling the Saffman-Taylor instability is grounded in the principles of mass and momentum conservation, coupled with Darcy's law and interfacial dynamics. The governing equations are derived as follows:

Navier-Stokes Equations and Simplifications

The Navier-Stokes equations for incompressible flow is:

$$\rho\left(\frac{\partial \mathbf{u}}{\partial t} + \mathbf{u}\cdot\nabla\mathbf{u}\right) = -\nabla P + \mu\nabla^2\mathbf{u} + \mathbf{f},$$

where ρ is the fluid density, $\mathbf{u}$ is the velocity field, P is pressure, μ is dynamic viscosity, and $\mathbf{f}$ is the body force.

For flow in a Hele-Shaw cell, with gap height $h \ll L$ (where L is the characteristic length in the x- and y-directions), the assumptions include:

- Steady, incompressible flow ($\partial\mathbf{u}/\partial t = 0$),
- Dominance of viscous forces (Re $\ll 1$),
- Neglect of inertial terms,
- Two-dimensional flow due to the thin gap height.

Integrating over the gap height under these assumptions, the Navier-Stokes equations reduce to Darcy's Law:

$$\mathbf{u} = -\frac{k}{\mu}\nabla P,$$

where $k = h^2/12$ is the permeability of the Hele-Shaw cell.

Laplace's Equation

The incompressibility condition $\nabla\cdot\mathbf{u} = 0$ leads to Laplace's equation for pressure:

$$\nabla^2 P = 0.$$

Boundary Conditions

At the fluid interface, the Laplace-Young condition governs the pressure jump due to surface tension:

$$P_{\text{inner}} - P_{\text{outer}} = \gamma\kappa,$$

where γ is the surface tension and κ is the interface curvature. In polar coordinates, the curvature is given by:

$$\kappa = \frac{1}{R} + \frac{\partial^2 R}{\partial\theta^2}.$$

Additional boundary conditions are:

- $P = P_{\text{interface}}$ at the inner boundary,
- $P = 0$ at the outer boundary.

Linear Stability Analysis

To analyze the instability, perturbations are introduced to the radial interface:

$$R(\theta, t) = R_0 + \epsilon\eta(\theta, t),$$

where R_0 is the unperturbed radius, $\epsilon \ll 1$ is the perturbation amplitude, and $\eta(\theta, t) = N(t)\cos(m\theta)$ is the perturbation mode with wave number m.

Substituting this perturbed radius into Darcy's Law, retaining terms up to first order in ϵ, and applying the Laplace-Young boundary condition, the growth rate of the perturbation is derived:

$$\sigma = \frac{v_{\text{injection}} m}{R_0} - \frac{\gamma m^3}{\mu R_0^2},$$

where $\sigma > 0$ indicates unstable growth, leading to fingering patterns, and $\sigma < 0$ corresponds to stabilization.

The critical wave number m_c that maximizes σ is:

$$m_c = \sqrt{\frac{\mu v_{\text{injection}}}{\gamma R_0}},$$

and the corresponding critical wavelength λ_c is:

$$\lambda_c = \frac{2\pi R_0}{m_c}.$$

Dimensionless Parameters

The capillary number (Ca), which governs the balance of viscous and surface tension forces, is defined as:

$$\text{Ca} = \frac{\mu v_{\text{injection}}}{\gamma}.$$

This parameter plays a critical role in determining the onset and characteristics of the instability.

5.2 Numerical Modeling[1]

A finite-difference numerical method is employed to simulate the Saffman-Taylor instability. The simulation involves solving Laplace's equation for pressure and updating the interface according to Darcy's law.

Numerical Methodology

1. **Grid Definition:** A Cartesian grid of size 200×200 is created with uniform spacing $\Delta x = \Delta y = 0.1$. The inner boundary is initialized as a perturbed circle:

$$R_{\text{inner}}(\theta) = R_0 + A\sin(m\theta),$$

where R_0 cm is the mean radius, A cm is the perturbation amplitude, and m is the mode number. The outer boundary is a fixed circle with radius R_{outer}.

2. **Pressure Solver:** Laplace's equation for pressure is solved iteratively using the Gauss-Seidel method:

$$P_{i,j} = \frac{1}{4}\left(P_{i+1,j} + P_{i-1,j} + P_{i,j+1} + P_{i,j-1}\right).$$

Boundary conditions are applied (for the interface to grow):

- $P_{\text{inner}} = 1.0$ at the inner boundary.
- $P_{\text{outer}} = 0.0$ at the outer boundary.

3. **Interface Evolution:** The pressure gradient is computed using central differences:

$$\frac{\partial P}{\partial x}, \frac{\partial P}{\partial y}.$$

Darcy's law updates the radial velocity:

$$v_r = -\frac{\gamma}{\mu}\sqrt{\left(\frac{\partial P}{\partial x}\right)^2 + \left(\frac{\partial P}{\partial y}\right)^2}.$$

The inner boundary radius evolves as:

$$R_{\text{inner}}(t + \Delta t) = R_{\text{inner}}(t) + v_r \Delta t.$$

The time step is $\Delta t = 0.01$ seconds.

4. **Visualization:** The results are visualized at regular intervals using contour plots for pressure and boundary overlays.

Simulation Challenges

The simulation accurately captures initial fingering patterns but diverges at longer times due to:

- Insufficient resolution near the boundaries, which limits the accuracy of pressure gradient calculations.
- Computational constraints preventing the use of smaller time steps and finer grids.
- For a larger time, the results of the program do not create real fingers; one of the reasons this is happening is because of the unavailability of points to simulate actual growth further on (In between the boundaries) and when tried to increase the size, the time is taken by the simulation to run too long with small time step due to which the calculations for pressure and velocities are incorrect.

5.3 Diffusion-Limited Aggregation (DLA) Modeling [2]

Our very simplified simulation is based on many DLA models of viscous fingering. After reviewing many articles ([3], [4], [5], [6], [7]), we noted that a great many studies of viscous fingering use DLA. However, several studies do not use DLA (for example, network models). A comprehensive review published in 2021 concluded that there is not yet a consensus on which mathematical model best simulates viscous fingering.

The review highlighted that the Navier-Stokes equations, or other equations for immiscible displacements, are commonly assumed in successful simulations and experiments. However, several studies indicated violations of Darcy's law, advised against relying on it, or suggested modifications, such as incorporating the Brinkman term. Some articles suggested that the Darcy law and DLA are not incompatible, while others pointed out the limitations of Darcy's law.

By contrast with these sophisticated models, we aimed to provide a brief introduction using simplified DLA models implemented in Scratch, Python, and NetLogo. These models use basic principles of stochastic aggregation to illustrate viscous fingering patterns.

5.4 Why We Use DLA Instead of Normal Algorithms

A simplified DLA approach is implemented to simulate viscous fingering as a stochastic aggregation process. Particles are released randomly and allowed to undergo a random walk until they adhere to the growing cluster. The sticking probability and seed radius are adjusted to mimic viscous fingering patterns. **Key assumptions in the DLA model include:**

- Particles are discrete and undergo Brownian motion.
- Aggregation occurs when particles are adjacent to the cluster.
- Surface tension effects are implicit in the sticking probability.

While DLA models provide qualitative insights into pattern formation, they lack the physical rigor of continuum-based approaches like Darcy's law.

Parameters and Variables

The following parameters and variables are defined for the DLA simulation:

- **Grid Size (`grid_size`):** The size of the simulation grid.
- **Number of Particles (`num_particles`):** Total number of particles used in the aggregation process.
- **Seed Radius (`seed_radius`):** The radius of the initial seed at the center of the grid.
- **Stick Probability (`stick_probability`):** Probability that a particle will adhere to the growing structure upon contact.

- **Grid (`grid`):** A boolean array of size `grid_size`×`grid_size` representing the simulation space.
- **Random Walk:** The stochastic motion of particles, implemented as a movement in one of four directions: up, down, left, or right.
- **Smoothing (`sigma`):** A Gaussian smoothing parameter applied post-simulation to improve visualization.

Software: The numerical simulations are implemented in Python using `numpy` and `matplotlib` for computation and visualization, respectively.

6 Results and Analysis

The experimental observations and model predictions showed significant alignment, particularly in capturing the fingering patterns characteristic of the Saffman-Taylor instability. Both analytical and numerical models were able to replicate key trends observed during the experiments conducted with the Hele-Shaw cell.

6.1 Fingering Patterns

Experimental results confirmed that higher injection rates led to thinner, more numerous fingers, while lower injection rates resulted in fewer, wider fingers. Numerical simulations validated this behavior, showing how variations in parameters such as surface tension and viscosity influenced the instability.

6.2 Interface Evolution

Analytical solutions derived from Darcy's law predicted the evolution of the interface over time. These predictions matched well with experimental data, especially in the early stages of the instability.

6.3 Critical Parameters

The Capillary number (Ca), a ratio of viscous forces to surface tension, was calculated for various flow conditions. Experimental results showed a clear relationship between Ca and the patterns formed: higher Ca values produced sharper and more unstable fingers, while lower Ca values led to smoother and more stable interfaces.

6.4 Numerical Outputs

Numerical modeling using finite-difference methods provided pressure distribution profiles and interface evolution over time. These models captured the transition from circular interfaces to finger-like structures with reasonable accuracy. The addition of diffusion-limited aggregation (DLA) models provided

insights into stochastic growth processes, which qualitatively matched experimental observations of pattern irregularities.

The agreement between experimental results and theoretical/numerical models highlights the accuracy of the modeling approaches and confirms their ability to describe the Saffman-Taylor instability under controlled conditions.

7 Sensitivity Analysis

Sensitivity analysis evaluates the impact of varying key parameters on the results of the numerical and diffusion-limited aggregation (DLA) simulations. This section systematically analyzes how changes in the input parameters affect the stability, pattern formation, and accuracy of the models.

The numerical simulation is governed by several parameters: surface tension (γ), viscosity (μ), grid resolution ($\Delta x, \Delta y$), time step (Δt), injection velocity ($v_{\text{injection}}$), and perturbation amplitude (A). The sensitivity of the system is analyzed with respect to these parameters.

Surface Tension (γ)

Surface tension stabilizes the interface, resisting the growth of perturbations. Increasing γ:

- Reduces the growth rate of fingering instabilities, as seen from the term $-\frac{\gamma m^3}{\mu R_0^2}$ in the growth rate equation.
- Results in fewer, wider fingers at the interface.

Decreasing γ has the opposite effect, leading to sharper, more unstable finger-like patterns.

Viscosity (μ)

Viscosity influences the damping of perturbations. Higher viscosity:

- Increases resistance to flow, slowing down interface evolution.
- Reduces the critical wave number $m_c = \sqrt{\frac{\mu v_{\text{injection}}}{\gamma R_0}}$, resulting in thicker fingers.

Lower viscosity increases the formation of narrower fingers but can lead to numerical instability.

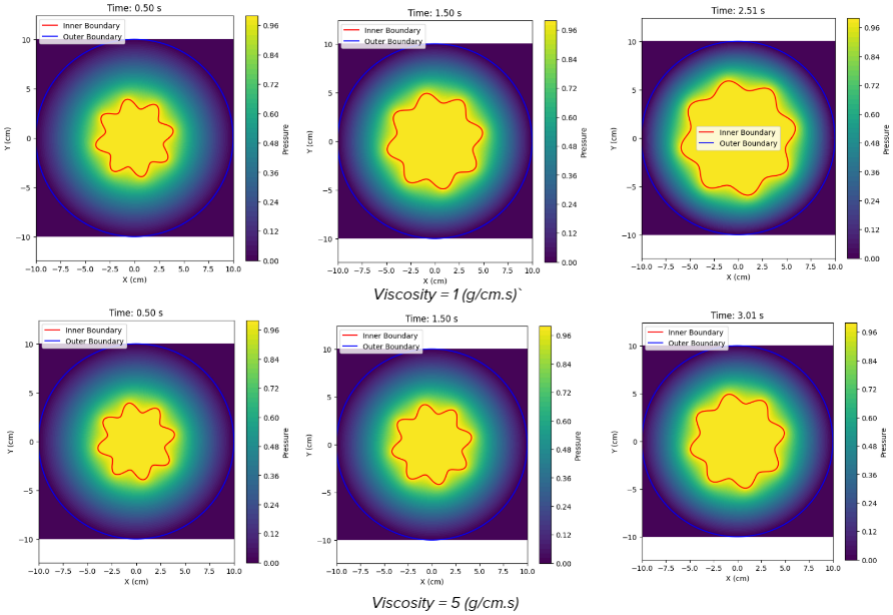

Figure 6: Change in Model when Viscosity is varied.

Grid Resolution ($\Delta x, \Delta y$)

A finer grid resolution:

- Improves the accuracy of the pressure gradient (∇P) calculation using finite differences.
- Resolves smaller-scale features of the fingering pattern but significantly increases computational cost.

Coarser grids fail to capture the fine structure of the interface, leading to unrealistic smoothing of the fingers.

Time Step (Δt)

A smaller Δt ensures stability of the numerical scheme but increases simulation time. Larger time steps:

- Can lead to numerical divergence, particularly for high perturbation modes ($m > m_c$).
- Introduce errors in the evolution of the interface, distorting fingering patterns.

Injection Velocity ($v_{\text{injection}}$)

Higher injection velocity accelerates the growth of fingers:

- Increases the growth rate term $\frac{v_{\text{injection}} m}{R_0}$, favoring the formation of higher wave number modes.
- Leads to thinner, more unstable fingers for high velocities.

Lower velocities produce wider, more stable fingers, as observed experimentally.

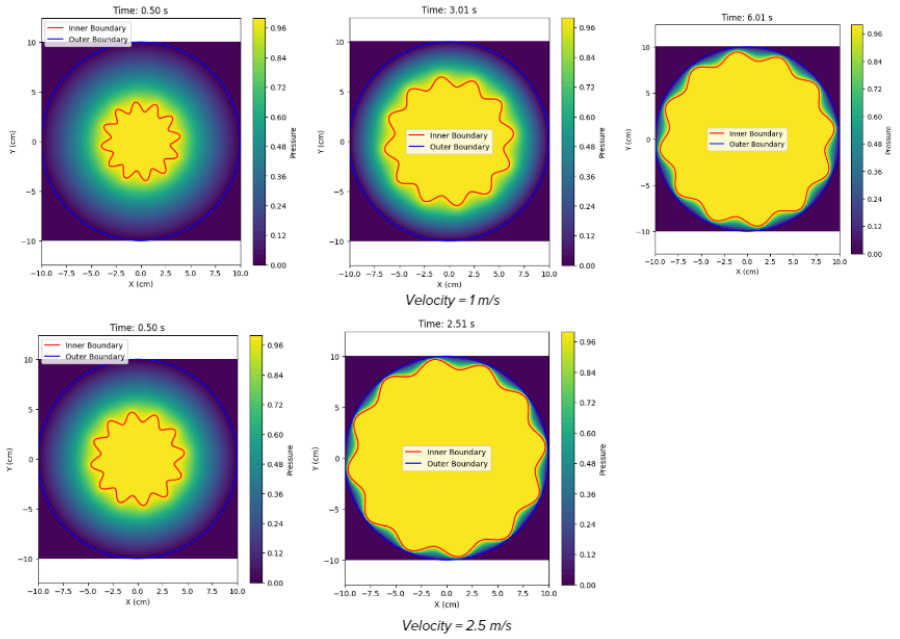

Figure 7: Change in Model when changing Injection Velocity.

Perturbation Amplitude (A)

The initial amplitude of perturbations influences the onset of instability:

- Larger A accelerates the nonlinear growth of fingers.
- Smaller A delays the emergence of fingering patterns, resulting in a more circular interface.

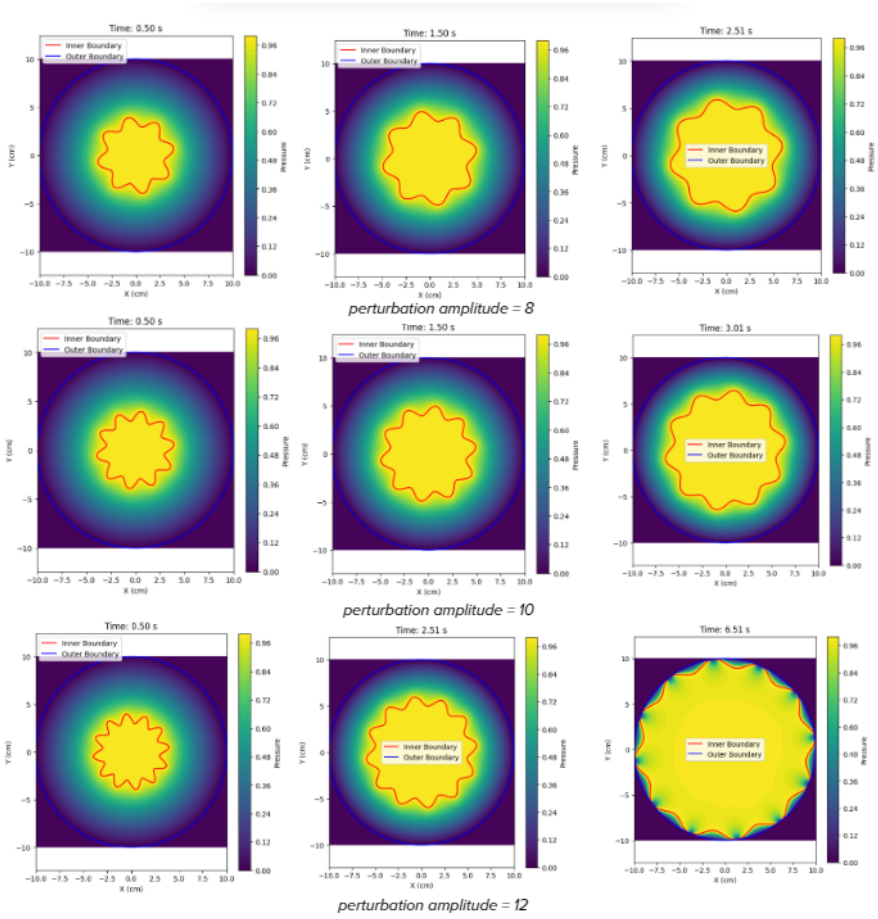

Figure 8: Change in Model when changing Perturbation Amplitude.

7.1 DLA Simulation Sensitivity Analysis

The DLA simulation depends on parameters such as grid size (grid_size), number of particles (num_particles), seed radius (seed_radius), and stick probability (stick_probability). Each parameter's influence on the fractal growth pattern is detailed below.

Grid Size (grid_size)

Larger grid sizes:

- Allow more extensive growth of the DLA structure, producing detailed fractal patterns.

- Increase computational time due to larger domains for particle simulation.

Smaller grids limit the growth and can cause artificial boundary effects.

Number of Particles (num_particles)

The number of particles determines the complexity of the aggregated structure:

- Increasing num_particles enhances the fractal detail and depth of the DLA pattern.
- Decreasing num_particles produces incomplete patterns with sparse growth.

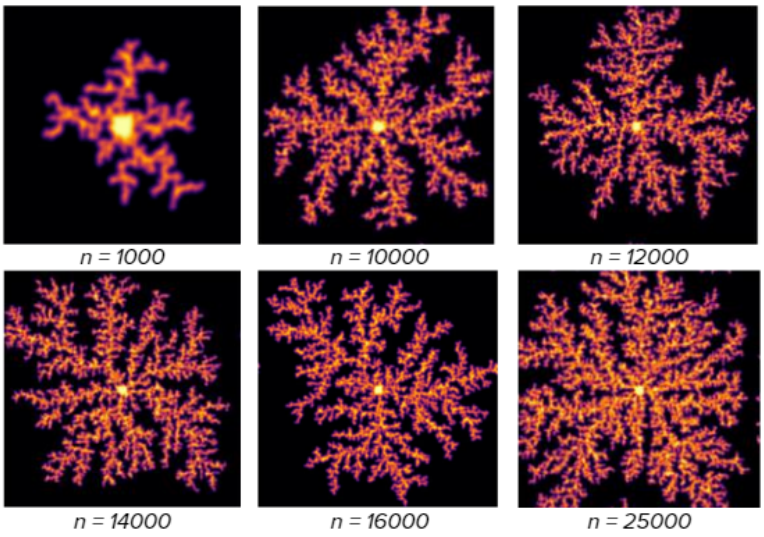

Figure 9: DLA model for various numbers of particles.

Seed Radius (seed_radius)

The seed radius sets the initial aggregation region:

- Larger seed radii produce broader initial clusters, reducing the fractal nature of the final pattern.
- Smaller radii enhance the fractal characteristics by allowing particles to aggregate more irregularly.

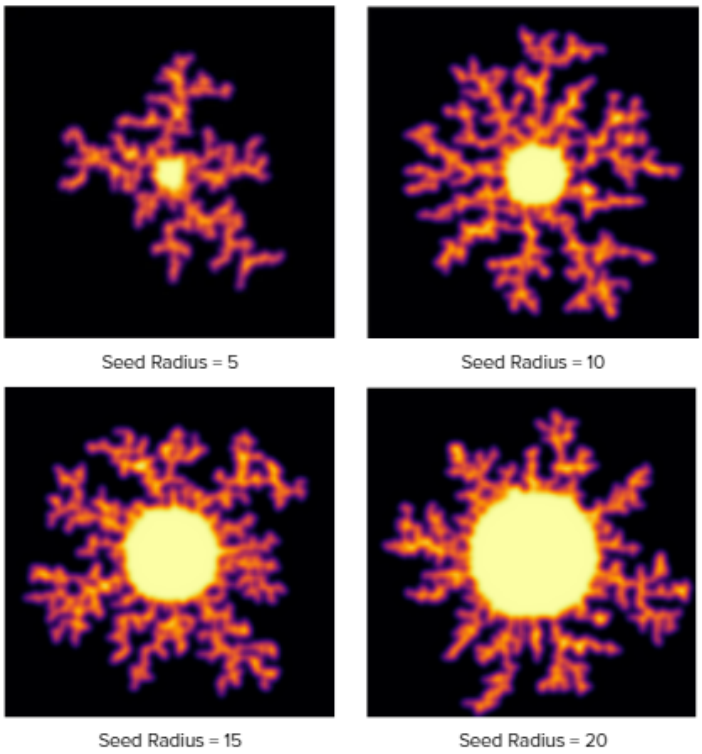

Figure 10: DLA model for different seed radius.

Stick Probability (stick_probability)

The stick probability governs the likelihood of particle adhesion:

- Higher stick_probability produces denser, more connected patterns.
- Lower stick_probability results in sparse, fragmented growth, potentially disrupting the fractal structure.

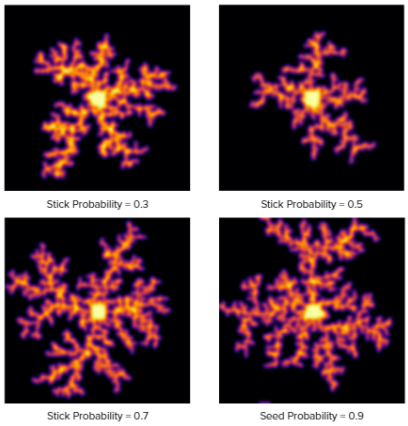

Figure 11: DLA model for different seed radius.

Smoothing (σ)

Gaussian smoothing (σ) is applied for visualization:

- Larger σ smooths fine details, obscuring the fractal features.
- Smaller σ retains sharpness, highlighting irregularities in the structure.

7.2 Comparison of Sensitivity Across Models

- The numerical model is highly sensitive to physical parameters such as γ, μ, and $v_{\text{injection}}$, directly influencing the stability and morphology of fingering patterns.
- The DLA model is more computationally sensitive, with grid size and particle count significantly affecting the fractal growth process.
- Both models emphasize the importance of resolution (grid spacing and particle density) in capturing the characteristic patterns of viscous fingering.

8 Discussions and Conclusion

The experimental and modeling efforts provided a comprehensive understanding of the Saffman-Taylor instability:

8.1 Key Insights

- The interplay between surface tension, viscosity, and injection velocity governs the formation of finger-like patterns at the fluid interface.
- Numerical simulations effectively captured the transition from stable interfaces to instability, validating theoretical predictions based on Darcy's law and linear stability analysis.
- Experimental observations confirmed the influence of the Capillary number and critical wavelength on instability dynamics.

8.2 Challenges and Limitations

- **Experimental Setup:** Irregularities in plate spacing, air bubbles, and manual injection rates introduced inconsistencies in pattern formation.
- **Numerical Models:** Long-term simulations diverged due to computational constraints, such as limited grid resolution and inaccuracies in boundary conditions.
- **Simplifications in Models:** While useful for predicting trends, analytical and numerical models lacked the ability to account for complex real-world factors like temperature variations and non-uniform viscosity distributions.

8.3 Potential Improvements

- Automating the injection system would reduce manual errors and provide more consistent results.
- Refining numerical models with adaptive meshing or higher-order solvers could enhance accuracy.
- Addressing experimental imperfections, such as eliminating air bubbles and ensuring uniform plate spacing, would improve data quality.

In conclusion, the study successfully demonstrated the mechanisms of the Saffman-Taylor instability and validated theoretical predictions through experimental and numerical approaches.

9 Future Work

To build on the current findings, several avenues for future work are proposed:

9.1 Model Refinement

- Develop three-dimensional models to capture additional complexities, such as vertical flow effects.
- Include temperature-dependent viscosity changes to simulate thermal effects on instability.

9.2 Experimental Enhancements

- Introduce automated injection systems and high-speed imaging to capture transient dynamics more accurately.
- Experiment with different fluid combinations to study a wider range of viscosity and surface tension contrasts.

9.3 Alternative Approaches

- Use advanced computational methods, such as lattice Boltzmann models (LBM), to simulate small-scale interactions at the fluid interface.
- Apply machine learning techniques to predict pattern evolution under varying conditions.

Application-Oriented Studies

- Investigate practical applications of the Saffman-Taylor instability, such as its role in enhanced oil recovery or fluid transport in porous materials.
- Explore the effects of instability in confined geometries, such as microfluidic devices.

By addressing these areas, future research can deepen our understanding of interfacial instabilities and extend the findings to broader scientific and engineering applications.

Bibliography

[1] "Kondic, L. (n.d.). Saffman-Taylor Instability [Math-451H]. https://web.njit.edu/~kondic/capstone/2015/saffman-taylor.pdf"

[2] "Arnéodo, A., Couder, Y., Grasseau, G., Hakim, V., Rabaud, M. (1989). Uncovering the analytical Saffman-Taylor finger in unstable viscous fingering and diffusion-limited aggregation. Physical Review Letters, 63(9), 984–987. https://doi.org/10.1103/physrevlett.63.984

[3] "Tian Wie, Peichao Li, Yaoge Liu, Zhiwei Lu. (2018). The simulation of viscous fingering by using a diffusion-limited-aggregation model during CO2 Flooding." Journal of Porous Media 21" https://www.researchgate.net/publication/326132280_The_simulation_of_viscous_fingering_by_using_a_diffusion-limited-aggregation_model_during_CO2_Flooding

[4] "Andrés Pinilla, Miguel Asuaje, Nicolás Ratkovich. (2021). "Experimental and computational advances on the study of Viscous Fingering: An umbrella review." Heliyon 18;7(7):e07614 (reviews many computational and experimental studies over 30 years, starting from the 1980s) https://www.sciencedirect.com/science/article/pii/S2405844021017175

[5] "Paterson, L. (1984). Diffusion-Limited Aggregation and Two-Fluid Displacements in Porous Media. Physical Review Letters, 52(18), 1621–1624. https://doi.org/10.1103/physrevlett.52.1621

[6] "Witten, T. A., Sander, L. M. (1981). Diffusion-Limited Aggregation, a Kinetic Critical Phenomenon. Physical Review Letters, 47(19), 1400–1403. https://doi.org/10.1103/physrevlett.47.1400

[7] "Løvoll, G., Jankov, M., Måløy, K. J., Toussaint, R., Schmittbuhl, J., Schäfer, G., Méheust, Y. (2010). Influence of Viscous Fingering on Dynamic Saturation–Pressure Curves in Porous Media. Transport in Porous Media, 86(1), 305–324. 8https://doi.org/10.1007/s11242-010-9622-"

[8] "Shokri, H., Kayhani, M., Norouzi, M. (2017b). Saffman–Taylor instability of viscoelastic fluids in anisotropic porous media. International Journal of Mechanical Sciences, 135, 1–13. https://doi.org/10.1016/j.ijmecsci.2017.11.008"

[9] "Norouzi, M., Yazdi, A., Birjandi, A. (2018). A numerical study on Saffman-Taylor instability of immiscible viscoelastic-Newtonian displacement in a Hele-Shaw cell. Journal of Non-Newtonian Fluid Mechanics, 260, 109–119. https://doi.org/10.1016/j.jnnfm.2018.06.007"

[10] "Lastra, Y., Moulton, L., Anazco, R., Kondic, L. (2014). THE HELE SHAW CELL/ SAFFMAN TAYLOR INSTABILITY: Theoretical and Experimental Comparison of Newtonian Fluids. https://web.njit.edu/~kondic/capstone/2015/2014_final_reports/451FinalReport.pdf"

1 Simulation Codes

1.1 Code for Modelling and Simulation Using Algorithm from Research Paper

```python
import numpy as np
import matplotlib.pyplot as plt

Nx, Ny = 200, 200  # grid size (increase for higher resolution)
dx, dy = 0.1, 0.1  # grid spacing
dt = 0.01  # time step
t_max = 3.0  # total simulation time
gamma = 72.8  # surface tension (dynes/cm)
mu = 1.0  # viscosity (g/(cm*s))
injection_velocity = 1.0  # injection velocity (cm/s)

x = np.linspace(-Nx // 2, Nx // 2, Nx) * dx
y = np.linspace(-Ny // 2, Ny // 2, Ny) * dy
X, Y = np.meshgrid(x, y)
R = np.sqrt(X**2 + Y**2)

theta = np.linspace(0, 2 * np.pi, 360)
inner_radius = 3.0
perturbation_amplitude = 0.5
perturbation_mode = 8
inner_boundary = inner_radius + perturbation_amplitude * np.sin(perturbation_mode * theta)

outer_radius = 10.0

pressure = np.zeros((Nx, Ny))

def solve_laplace(pressure, inner_mask, outer_mask):
    for _ in range(500):  # Iterative Gauss-Seidel solver
        pressure[1:-1, 1:-1] = 0.25 * (
            pressure[:-2, 1:-1] + pressure[2:, 1:-1] +
            pressure[1:-1, :-2] + pressure[1:-1, 2:]
        )
        pressure[inner_mask] = 1.0
        pressure[outer_mask] = 0.0
    return pressure

time = 0.0
while time < t_max:
    inner_boundary = inner_radius + perturbation_amplitude * np.sin(perturbation_mode * theta)
    x_inner = inner_boundary * np.cos(theta)
    y_inner = inner_boundary * np.sin(theta)

    inner_mask = np.zeros_like(R, dtype=bool)
    for xi, yi in zip(x_inner, y_inner):
      inner_mask |= (np.sqrt((X - xi)**2 + (Y - yi)**2) < dx)

    outer_mask = (np.abs(R - outer_radius) < dx)

    pressure = solve_laplace(pressure, inner_mask, outer_mask)

    grad_P_x, grad_P_y = np.gradient(pressure, dx, dy)

    radial_velocity = -gamma / mu * np.sqrt(grad_P_x**2 + grad_P_y**2)
    inner_radius += injection_velocity * dt

    time += dt

    if int(time / dt) % 50 == 0:
        plt.figure(figsize=(6, 6))
        plt.contourf(X, Y, pressure, levels=50, cmap='viridis')
        plt.colorbar(label="Pressure")
        plt.plot(x_inner, y_inner, 'r-', label='Inner Boundary')
        plt.plot(outer_radius * np.cos(theta), outer_radius * np.sin(theta), 'b-', label='Outer Boundary')
        plt.legend()
        plt.title(f"Time: {time:.2f} s")
        plt.xlabel("X (cm)")
        plt.ylabel("Y (cm)")
        plt.axis('equal')
        plt.show()

print("Simulation complete.")
```

Listing 1: Numerical Simulation Code Based on Research Paper

1.2 Code for Modelling and Simulation Using DLA Algorithm

```
import numpy as np
import matplotlib.pyplot as plt
from scipy.ndimage import gaussian_filter

grid_size = 100
num_particles = 1000
seed_radius = 5
stick_probability = 0.5

grid = np.zeros((grid_size, grid_size), dtype=bool)

center = grid_size // 2
y, x = np.ogrid[-center:grid_size-center, -center:grid_size-center]
mask = x**2 + y**2 <= seed_radius**2
grid[mask] = True

def random_walk(x, y):
    direction = np.random.choice(['up', 'down', 'left', 'right'])
    if direction == 'up':
        y = (y - 1) % grid_size
    elif direction == 'down':
        y = (y + 1) % grid_size
    elif direction == 'left':
        x = (x - 1) % grid_size
    elif direction == 'right':
        x = (x + 1) % grid_size
    return x, y

def is_adjacent(x, y):
    adjacent = grid[(x-1)%grid_size, y] or grid[(x+1)%grid_size, y] or \
               grid[x, (y-1)%grid_size] or grid[x, (y+1)%grid_size]
    return adjacent

for _ in range(num_particles):
    x, y = np.random.randint(0, grid_size, 2)
    while True:
        x, y = random_walk(x, y)
        if is_adjacent(x, y):
            if np.random.rand() < stick_probability:
                grid[x, y] = True
                break

smoothed_grid = gaussian_filter(grid.astype(float), sigma=1.0)

plt.figure(figsize=(8, 8))
plt.imshow(smoothed_grid, cmap='inferno', interpolation='bilinear')
plt.axis('off')
plt.show()
```

Listing 2: Diffusion-Limited Aggregation Simulation Code